

Publication VIII

Minna Toivola, Marju Ferenets, Peter Lund, and Ali Harlin. 2009. Photovoltaic fiber. *Thin Solid Films*, volume 517, number 8, pages 2799-2802.

© 2008 Elsevier Science

Reprinted with permission from Elsevier.



## Photovoltaic fiber

Minna Toivola <sup>a</sup>, Marju Ferenets <sup>b,\*</sup>, Peter Lund <sup>a</sup>, Ali Harlin <sup>b</sup>

<sup>a</sup> Advanced Energy Systems, Department of Applied Physics, Helsinki University of Technology, P.O. Box 5100, 02015 TKK, Finland

<sup>b</sup> Laboratory of Fiber Materials Science, Department of Materials Science, Tampere University of Technology, Korkeakoulunkatu 6, 33720, Tampere, Finland

### ARTICLE INFO

#### Article history:

Received 21 June 2008

Received in revised form 30 October 2008

Accepted 3 November 2008

Available online 13 November 2008

#### Keywords:

Dye sensitized solar cell

Optical fiber

Optoelectronic device

### ABSTRACT

The optoelectronically active optical fiber is demonstrated in this work. This fiber consists of dye sensitized solar cell (DSC) structure deposited on claddingless optical fiber. Both silica and plastic optical fibers are used as a substrate. Such a fiber converts light modes propagating in the modified cladding into electrical signal. DSC structure consisting of ZnO:Al transparent current collector layer, TiO<sub>2</sub> photoelectrode sensitized with ruthenium dye, gelatinized iodine electrolyte, and carbon-based counter electrode was deposited layer by layer on top of the optical fiber. Current density–voltage curves of photovoltaic (PV) fibers of different diameters are presented. Maximum obtained short circuit current,  $I_{sc}$ , was 26 nA/cm<sup>2</sup> and maximum open circuit voltage,  $V_{oc}$ , was 0.44 V. The fabrication issues and applications of the PV fiber are discussed in the article.

© 2008 Elsevier B.V. All rights reserved.

### 1. Introduction

Fibrous optoelectronic structures have been an attractive area of research for various applications. The advantages of fiber devices include, for instance, flexibility, light weight, and possibility to make large area active surfaces that can be incorporated in wearable technology. Integrated self-monitoring optical transport fiber has been developed consisting of a photonic band gap optical fiber and temperature monitoring elements along the entire fiber length [1]. A tunable fiber photodetector has been made comprising an amorphous semiconductor core contacted by metallic nanowires, and surrounded by a cylindrical-shell resonant optical cavity. Such fibers have been arranged in a form of “spectrometric fabric” [2]. Also, an optical fiber based organic photovoltaic (PV) device using poly(3-hexylthiophene) and 1-(3-methoxycarbonyl)-propyl-1-phenyl-(6,6)C<sub>61</sub> bulk heterojunction blends as the absorbing material has been fabricated onto multimode optical fiber [3].

Powering wearable and implantable electronic devices remains still a problem in the fields of smart textiles and medical applications, for example. PV optical fiber comprising a PV cell build around the core of an optical fiber would enable to produce electricity over optical fiber to electronic devices that are situated in remote and/or confined places. The size and weight of an optical fiber compared to electrical cable is much smaller and the transmission distance can be longer. The use of optical fibers instead of metal cables would be especially favorable in harsh environments, where there is a problem of electromagnetic interference, or where sparks or shorts can be a fatal problem. It could also be used in sensor applications as an in-line photodetector.

Low-cost materials, wide range of applications and simple manufacturing process make nanostructured dye-sensitized solar cells (DSC) [4] a potential alternative to the traditional silicon and thin film PV devices. Unlike crystalline semiconductor solar cells, DSC is an electrochemical device, consisting of two electrodes interconnected by a layer of redox electrolyte. Electricity is generated at the photoelectrode, which is a porous, high surface area network of TiO<sub>2</sub> nanoparticles, coated with a monolayer of light-absorbing dye and permeated with the electrolyte. High surface area of the film enables larger amount of dye molecules to adsorb on TiO<sub>2</sub>, thus increasing the photocurrent the cell is able to generate. Photoexcitation of the dye molecules, a process mimicking nature's photosynthesis reaction, leads to injection of the excited electrons into the TiO<sub>2</sub> conduction band, from which they can be directed to an external circuit through the conductive substrate working as the current collector. The function of the redox electrolyte is to transport the positive charge created in the photoexcitation process to the counter electrode (CE) where it, in turn, gets reduced by the electrons returning from the external load. In short, the cell operation is based on consecutive oxidation-reduction cycles and no chemical substances get permanently transformed or consumed in the cell processes. Fig. 1 presents the operating principle of the DSC.

DSC electrodes are typically deposited on conducting glass, but to enable cost-efficient, roll-to-roll type large scale industrial manufacturing of the cells, alternative substrates such as light-weight and flexible plastic or metal materials have been studied extensively during the last few years. In this light, a DSC functioning as an optoelectronically active cladding on an optical fiber is an interesting concept. Fibrous CuI-based solid state DSC has been demonstrated using a metal wire as the photoelectrode substrate [5], but the conventional, iodine electrolyte DSC fabricated on optical fiber has not been reported before. The aim of this work is to prepare and characterize PV optical fiber based on the DSC technique.

\* Corresponding author.

E-mail address: [marju.ferenets@tut.fi](mailto:marju.ferenets@tut.fi) (M. Ferenets).

## 2. Experimental details

### 2.1. Preparation of the optical fiber DSC

Two types of fibers were used: polymethylmethacrylate (PMMA) (Baltronic Oy), diameter 1.3–2.0 mm and glass (Photonium Oy), diameter 1.0–1.5 mm. All fibers were claddingless, and made electrically conductive by coating 130 nm of ZnO:Al on them with atomic layer deposition (ALD) technique using the Beneq P400 equipment.

The standard procedure to prepare nanoporous, high surface area photoelectrode films for DSC consists of two steps. First, the TiO<sub>2</sub> is deposited on the substrate, typically in a form of paste or solution containing TiO<sub>2</sub> nanoparticles. In the second step dry film of TiO<sub>2</sub> is sintered at 450–500 °C for 30 min to ensure proper necking between the particles and to improve the film's adhesion to the substrate. The maximum temperature the PMMA fiber can withstand is, however, only 85 °C, which renders sintering of the photoelectrodes impossible in this case. Mechanical compressing is a technique often used to manufacture nanoporous TiO<sub>2</sub> layers at low temperatures, but it is problematic to be implemented in case of thin, cylindrical fibers. This is why, on PMMA fibers, the photoelectrode consisting of 50 nm of TiO<sub>2</sub> was prepared with the ALD method too.

Glass fibers tolerate temperatures needed for sintering, which enabled preparation of porous photoelectrodes on them. Commercial TiO<sub>2</sub> paste (Sustainable Technologies International) was diluted with terpineol to make it fluid enough for dip-coating. One layer of TiO<sub>2</sub> was applied (additional dippings gave a too thick, flaking layer) and let dry at room temperature, after which the fibers were sintered at 475–500 °C for 30 min. After that the fibers were immersed in the dye solution consisting of 0.32 mM of the N-719 dye (cis-bis(isothiocyanato)bis(2,2'-bipyridyl-4,4'-dicarboxylato)-ruthenium(II) bis-tetrabutylammonium, Solaronix SA) in absolute ethanol for ca. 48 h. PMMA fibers with the nonporous TiO<sub>2</sub> layer were dyed in the same solution. Before dyeing, or, in the case of glass fibers, dip-coating the TiO<sub>2</sub>, the fibers were cleaned in ethanol in an ultrasonic bath and dried with warm air. After the sensitization period, excess dye was rinsed off with ethanol.

Gelatinized iodine electrolyte was added next, with dip-coating from hot solution (the electrolyte gel turns into liquid when heated to 120–130 °C, and solidifies quickly again at room temperature). The electrolyte composition was 0.5 M LiI, 0.05 M I<sub>2</sub> and 0.5 M 4-*tert*-butylpyridine in 3-methoxypropionitrile (MePRN), with 5 wt.%

polyvinylidene fluoride-hexafluoro-propylene (PVDF-HFP) added as the gelatinizing agent (a method described in the literature [6]).

Carbon-based counter electrode was coated the last. The counter electrode gel was prepared by grinding 1.4 g of graphite powder (synthetic, conducting grade, –325 mesh, by Alfa Aesar) and 0.4 g of carbon black (Printex XE2, extra-conducting grade, by Degussa) together in a mortar with 2 g of MePRN. After that, 0.72 g of TiO<sub>2</sub> nanoparticles (P25, Degussa) were added, ground again and finally, the mixture was made into thick suspension by adding 10 g of MePRN. The suspension was stirred vigorously overnight, a few grams of MePRN added the next day to ensure fluid enough composition, and gelatinized with 5 wt.% of PVDF-HFP. This composition of the counter electrode material is slightly modified from what has been previously described in the literature, and studied in our own laboratory as well [7]. Here, ethanol was replaced with MePRN as the solvent because the higher boiling point of the latter enables the use of PVDF-HFP as the gelatinizing agent. A gel where the carbon materials and TiO<sub>2</sub> were mixed with ethanol and gelatinized with ethylcellulose was also tested, but with unsatisfactory results (too brittle structure after solidification). Counter electrode was deposited by quick dip-coating from hot gel solution, analogously to the electrolyte layer. The gel made with MePRN and PVDF-HFP solidified into hard, sturdy coating on which the current collector contact was easy to attach.

Photoelectrode side current collector was made by attaching a small piece of copper or aluminum tape around the fiber and adding a few drops of conductive silver epoxy to reduce the contact resistance between the tape and the ZnO:Al coating. On the counter electrode side, the contact was made of a thin copper wire wrapped tightly around the fiber. Fig. 2 presents a schematic drawing and a photograph of the photovoltaic fibers. The structure of the ALD-deposited ZnO:Al conductive coating and nonporous TiO<sub>2</sub> as well as nanoporous TiO<sub>2</sub> films were studied with scanning electron microscopy (SEM).

### 2.2. Measurements

The performance of the optical fiber DSC was characterized with current density–voltage (*I*–*V*)–curve measurements in a solar simulator. Two solar simulators were used: first, a custom-built apparatus equipped with ten 150 W halogen lamps as the light source, a temperature-controlled measurement plate and a calibrated monocrystalline silicon reference cell with which the illumination could be adjusted to the

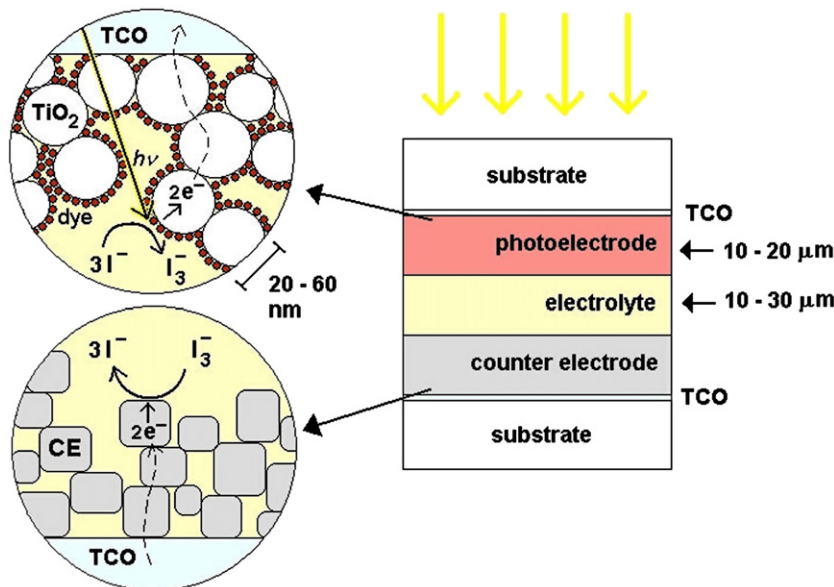


Fig. 1. Operating principle of the DSC.

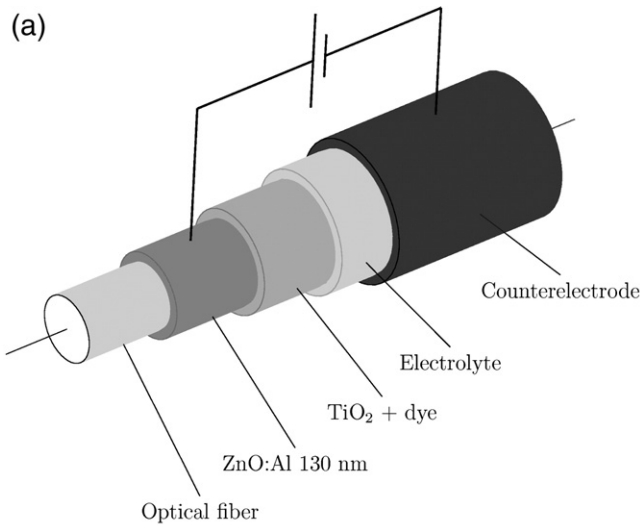


Fig. 2. (a) Schematic drawing of the PV fiber. (b) Photograph of the PV fibers (without the CE contacts) of different diameters.

standard 1000 W/m<sup>2</sup>. The spectral mismatch factor of the simulator, defined with the reference cell and the measured spectral irradiance of the halogen lamps was used to make the curves correspond with the standard AM1.5G equivalent illumination. The problem with this simulator was that, due to the lack of suitable light-concentrating optics and a pigtail fiber for guiding the illumination into the DSC fiber, the measurements had to be done using side lighting.

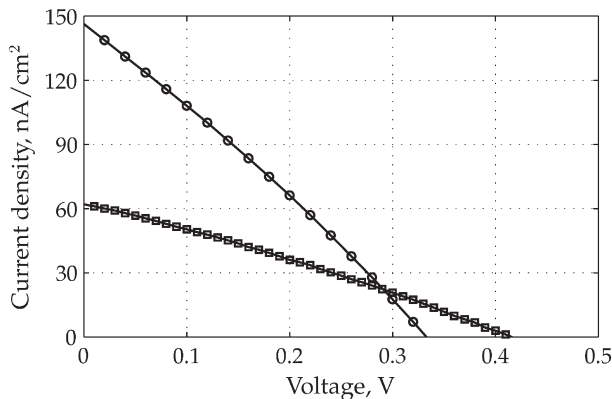


Fig. 3. Some examples of *I*–*V* curves measured for plastic optical fiber DSCs, lighting from the side.

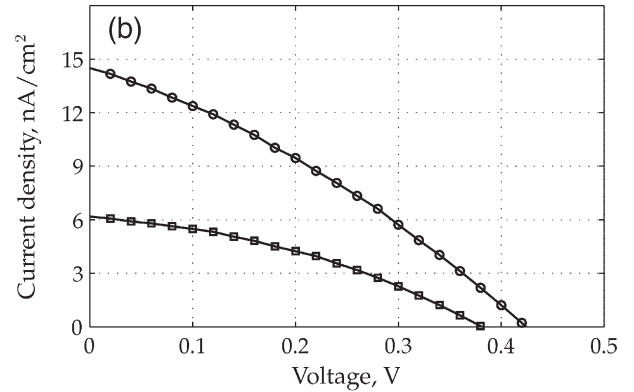
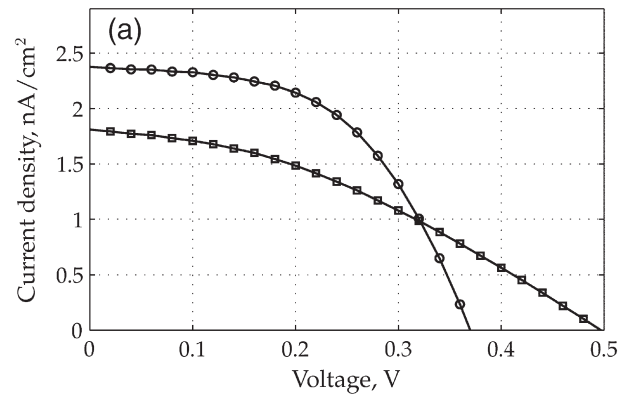


Fig. 4. Some examples of *I*–*V* curves measured for (a) glass and (b) plastic optical fiber DSCs, lighting from the inside.

While enough light to create a distinguishable voltage and current signal entered the fiber even from the side, this lighting geometry is not realistic considering the possible applications of these cells. This is why the fibers were measured also in a commercial simulator with a Xe-lamp (Newport, model 6247, 75 W XeHS) as the illumination source and coupling the light into the DSC fiber with a pigtail. After coupling losses, the power of the incident light at the end of the fiber was ca. 10 mW. Due to the evaporation of the electrolyte solvent, the fibers were prepared and the *I*–*V*-curves measured the same day.

### 3. Results and discussion

Typical *I*–*V*-curves of the PV optical fiber DSCs (See Fig. 2), measured with the lighting geometries described in Section 2.2 are presented in Figs. 3 and 4. Table 1 lists the following operating parameters of the cells: open circuit voltage (*V*<sub>oc</sub>), short-circuit current (*I*<sub>sc</sub>), fill factor (FF) and total power conversion efficiency (*η*). The highest measured open circuit

Table 1  
*I*–*V*-parameters of the optical fiber DSC

Type of fiber	Type of illumination	Fiber diameter (mm)	<i>V</i> <sub>oc</sub> (V)	<i>I</i> <sub>sc</sub> (nA/cm <sup>2</sup> )	FF (%)	<i>η</i> (%) × 10 <sup>−6</sup>
PMMA	From the side	1.5	0.33	146.0	28	N/A <sup>a</sup>
PMMA	From the side	1.5	0.42	62.0	29	N/A
Glass	From the inside	1.0	0.37	2.37	53	8.5
Glass	From the inside	1.2	0.50	1.81	36	7.2
PMMA	From the inside	1.5	0.42	14.5	31	53.7
PMMA	From the inside	1.3	0.38	6.18	37	22.4

<sup>a</sup> Because of the shadowing effect caused by the electrolyte and CE layers, approximating the incident light power density on the fiber active area is difficult when the light comes from the side, which is why the efficiencies of the side-lighted samples were not calculated. With samples illuminated from inside the fiber, the incident light power of 10 mW was approximated to spread evenly over the active area of the cell.

voltages of the cells were 0.50 V with side lighting, and 0.44 V with light coming from inside the fiber, which are not far from the values typically obtained with planar DSC geometry (0.6–0.7 V), using the same materials as the ones in this research. The most prominent characteristic of the cells was, however, their low short circuit current, though this can be easily understood considering the TiO<sub>2</sub> layer preparation technique. ALD method yields nonporous, compact films on which only a small amount of dye can be adsorbed, and this should show directly in the magnitude of the photocurrent.

Surprisingly however, glass fiber based DSCs had even lower performance. This is because the adhesion of the sintered, porous TiO<sub>2</sub> layer on the glass fibers was rather poor, and roughly half of the layer detached in the rinsing. Deposition method is most probably responsible for this: TiO<sub>2</sub> paste is typically applied by doctor-blading or screen-printing, which results in thin, even films the adherence of which to the substrate is better already before sintering because of the pressure applied while the paste is spread.

It is also possible that the surface energy and surface properties of SnO<sub>2</sub>:F, which is the typically used conductive coating on DSC glass substrates, are more favorable for TiO<sub>2</sub> adhesion, compared to those of ZnO:Al. The quality of the sintered and ALD-coated TiO<sub>2</sub> layers can be seen from the SEM images presented in Fig. 5.

Test results show that the best performance of PV fibers was achieved with side illuminated samples. This is easily explainable

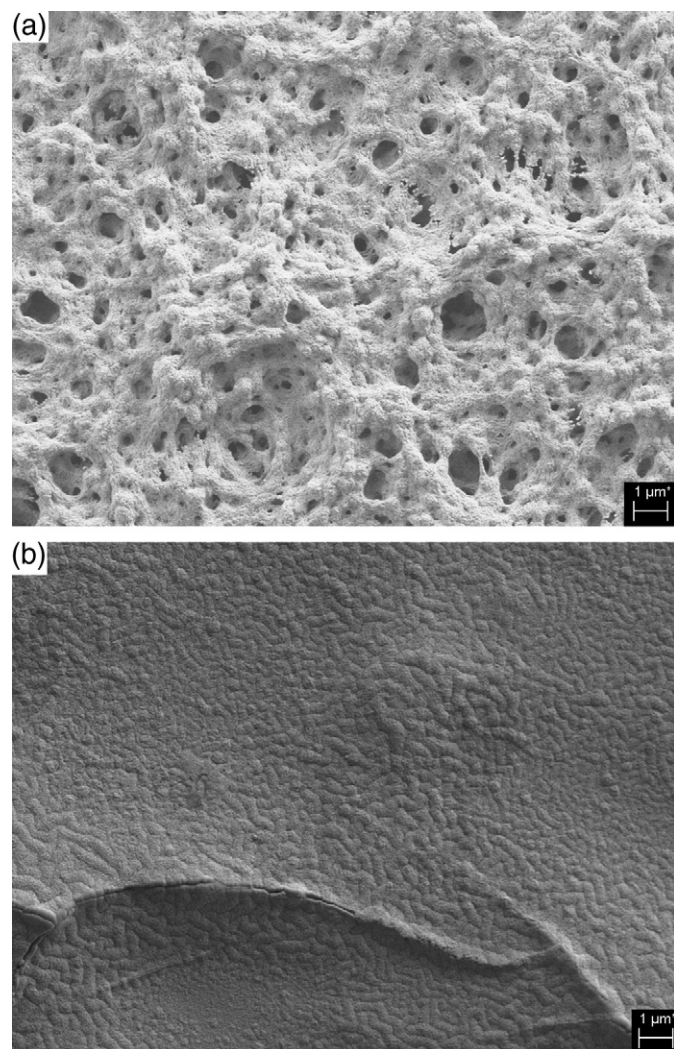


Fig. 5. Surface morphology of the photoelectrode: (a) Nanoporous TiO<sub>2</sub> on glass fiber; (b) ALD coating on PMMA fiber: 130 nm of ZnO:Al on the bottom, 50 nm TiO<sub>2</sub> on top.

though because in these fibers the opaque counter electrode paste was wiped off, while still soft, from that side of the fiber which faced the direction of the incoming light. Also, the light intensity in the simulator which the side illuminated samples were measured with was higher than what could be guided into the PV fiber with a pigtail fiber. This means that a larger amount of light was able to enter the photoactive area from the side than from inside the fiber, making the results obtained with these two different lighting geometries not directly comparable. Also, even if the side illumination is unrealistic considering how an optical fiber typically functions, it is “direct” and avoids the coupling losses which are bound to occur when light is directed to the PV fiber from a pigtail. Fiber diameter, on the other hand, did not have any influence on the fiber based DSC’s performance.

Even if the current (and thus, cell power and efficiency) is low, the cell voltage is clearly measurable, which enables the use of this kind of a DSC as an optoelectronic sensor, for example to monitor the propagation of light in the optical fiber. In the finished product, hermetic sealing of the DSC with a suitable encapsulant material is also needed, to prevent the electrolyte from drying (even if the gel is solid at room temperature, the polymer in it forms only a loose matrix around the electrolyte species and does not stop electrolyte evaporation over time) and moisture from penetrating into the cell. Developing such a material and application technique for it was beyond the scope of this research, though to overcome the problem with the electrolyte’s long-term stability, ionic liquid based gel was also studied. Here, MePRN was replaced with 1-methyl-3-propylimidazolium iodide (PMII) and the LiI concentration decreased from 0.5 M to 0.1 M. The rest of the electrolyte composition was the same as described earlier. Gelatinization of the ionic liquid turned out to be problematic, however. PVDF-HFP did not dissolve properly into PMII, and the resulting gel had poor adhesion on the fiber, which is why the studies were continued with the conventional iodine electrolyte gel.

#### 4. Conclusions

A photovoltaic optical fiber, where dye-sensitized solar cell structure functions as an optoelectronically active cladding, has been demonstrated. The maximum obtained open circuit voltage of this optical fiber DSC was 0.44 V with light coming from inside the fiber, and 0.50 V with side lighting. Due to the preparation technique and the resulting compact, nonporous structure of the TiO<sub>2</sub> photoelectrode film the maximum obtained short circuit current was 26 nA/cm<sup>2</sup>, which obviously yields only modest power conversion efficiencies. However, the open circuit voltage is almost as high as what is usually obtained with the typical, planar geometry DSC. This enables the use of this fiber-based DSC as an optically active sensor, for example, for monitoring the propagation of light in an optical fiber.

#### Acknowledgements

Financial support from the Finnish Funding Agency for Technology and Innovation (Tekes) is gratefully acknowledged. The authors thank Beneq, Inc. for the ALD-coatings and Dr. Vladimir Chukharev from the Institute of Chemistry, Tampere University of Technology for assistance in *I*–*V*-measurements.

#### References

- [1] M. Bayindir, O. Shapira, D. Saygin-Hinczewski, J. Viens, A.F. Abouraddy, J.D. Joannopoulos, Y. Fink, *Nat. Matters* 4 (2005) 820.
- [2] M. Bayindir, F. Sorin, A.F. Abouraddy, J. Viens, S.D. Hart, J.D. Joannopoulos, Y. Fink, *Nature* 431 (2004) 826.
- [3] J. Liu, M.A.G. Nambhothiry, D.L. Carroll, *Appl. Phys. Lett.* 90 (2007) 063501.
- [4] B. O’Regan, M. Gratzel, *Nature* 353 (1991) 737.
- [5] X. Fan, Z. Chu, L. Chen, C. Zhang, F. Wang, Y. Tang, J. Sun, D. Zou, *Appl. Phys. Lett.* 92 (2008) 113510.
- [6] P. Wang, S.M. Zakeeruddin, M. Gratzel, *J. Fluorine Chem.* 125 (2004) 1241.
- [7] J. Halme, M. Toivola, A. Tolvanen, P. Lund, *Sol. Energy Mater. Sol. Cells* 90 (2006) 872.